

.....

A New Technique to Control the Architecture of Neuronal Networks *in vitro*

Claire Wyart, Christophe Ybert, Carine Douarche, Catherine Herr, Didier Chatenay, Laurent Bourdieu

Laboratoire de Dynamique des Fluides Complexes, UMR 7506 CNRS, Université Louis Pasteur, Institut de Physique, Strasbourg, France

Introduction

Long-term studies of neuronal networks require observing the activity of interconnected neurons and their interactions. The motivation for these studies is varied: (1) testing the effect of a new agent on the interactions between neurons [1, 2]; (2) improving neuronal–electronic interfaces [3, 4] by placing the neuron soma on recording or stimulating electrodes; (3) studying the interactions between neurons during development [5–11].

Most approaches to understand information processing in biological neuronal networks use *in vivo* or brain slice preparations. A major advantage of these preparations lies in the fact that the development of neurons occurs in physiological conditions. Membrane properties and the architecture of synaptic connections between neurons are also preserved. However, in these systems, it is not possible to determine easily the functional architecture (inhibitory vs. excitatory nature of the neurons and their connectivity) of the neuronal network being studied. Neither is it possible to follow the activity at the single unit level of an assembly of interconnected cells (containing more than two neurons). The complex structure of these systems results in experimental limitations:

- (1) Despite the great advances in optical and electrophysiological techniques [12–14], it is not possible to record simultaneously the activity of all neurons in a network.
- (2) However, activity can be recorded by different techniques over a large number of neurons simultaneously [15]. Nevertheless, for more than two

neurons, the precise connectivity is not known and must be estimated from the timing of action potentials.

- (3) The respective contribution of synaptic, cellular, and network properties to neuronal network dynamics is in general difficult to analyze since they are often all involved simultaneously, for example, the case of reverberating excitation in a recurrent network [16].
- (4) The impact of synaptic noise on network dynamics, for example, the case of the initiation or maintenance of spontaneous activity, is difficult to evaluate since there are no methods to differentiate the synaptic noise from the synaptic response following cell activation while keeping the network activity intact.

In dissociated neuronal cell cultures in chemically defined medium [17, 18] the structural integrity of the tissue is lost, but a higher degree of biochemical and biophysical control is possible. For example, culture systems enable simultaneous recording of the activity of groups of three to four connected neurons in an isolated network [6, 19] and studying the long-term effect of the molecules applied in the medium [2]. However, in standard cultures, the random spatial distribution, the overlap of neurites, and the motion of neurons on the homogeneous substrate do not allow reaching a stable ordered state of the network over time and complicate the observation of a single neuron over a long period of time [20]. Moreover, the probability of synaptic contact between close neurons is low. Finally, the expression of certain neuronal properties, such as synaptic density or neurite growth, depends on the density of neurons in the culture [21].

Standard culture, therefore, has many drawbacks in studying the dynamic properties of neuronal networks. This matters in particular for studies related to the role of functional architecture in determining the transfer of information in a network: the synaptic connectivity of neurons in culture does not share any common properties with the *in situ* organization and does not even remain stable while *in vitro* since neurons are constantly moving on the substrate (especially after plating).

Limitations of the standard dissociated culture approach to studying neuronal networks leads us to develop a new method to control the network architecture *in vitro*. Photolithography, with adhesion patterns, has been used to select the location of neuronal cell bodies on glass coverslips and constrain the growth of neurites on defined axes. We will see in this article that the elaboration of these small closed networks of defined architecture (number of neurons and their position) provides a control on the synaptic connectivity.

These *in vitro* neuronal networks, obtained by confining soma location and neurite elongation to a predefined pattern, should allow circumventing classical difficulties and open a way to conduct experiments, which are not

currently possible. By immobilizing cell bodies in defined positions, this technique facilitates the study of individual neurons and of their interactions with their neighbors during the normal development of the network over weeks as well as after incubation with drugs [1, 2]. It may then be feasible to monitor and stimulate neuronal activity by forming artificial neuronal circuits using neuron to electronic interfaces [4, 22]. All these developments require that neurons fulfill four essential conditions: (1) long term conservation of growth pattern and low-density survival *in vitro*; (2) physiological integrity; (3) presence of both inhibitory and excitatory neurons; (4) maturity of synapses.

The realization of these adhesion patterns allows obtaining a wide diversity of structures depending on their size: from the most simple (the isolated neuron, called *autapse*), to the pluri-cellular networks. The structure of these neuronal networks has no similarity with the structure of *in vivo* neuronal networks. Nevertheless, the functional architecture of the network (number of neurons, presence of inhibitory neurons) can be characterized and remains identical over time. Therefore, if the neuronal physiology is conserved in culture, knowledge of the architecture of these isolated networks, formed *in vitro* during the maturation process, is a key element to address many problems in the fields of pharmacology, development and physiology.

Two main strategies, both based on lithography, have been used in the past to control the architecture of neuronal networks in culture: either guidance by 3D topography or guidance by spatial contrasts in the substrate's adhesive properties. The second method has been more successful [23–25]. For many years, different groups attempted to develop methods to control the organization of neuronal networks *in vitro* by spatial adhesion contrast. In these studies, the main objective was to fix the number of neurons in the network, to set the location of cell bodies to predefined sites (so that they do not move for days and weeks) and to guide the growth of the neurites, which may control the manner neurons connect to each other. Patterning technologies use mainly lithography and self-assembled monolayers [22, 23, 24–26]. Photolithographic protocols usually consist of grafting two silane molecules with antagonistic action on cellular growth onto glass slides with micron-scale resolution. Some growth-permissive molecules (e.g. an aminosilane or laminin-derived synthetic peptide) [27, 28] favor neuron adhesion and growth, whereas anti-permissive molecules such as fluorosilanes prevent it.

In these studies, several problems have emerged: (1) poor long-term (>1–2 weeks) survival of neurons; (2) decrease in the efficiency of neurite guidance after a few days of culture; (3) weak excitability of the neurons and little synaptogenesis. Indeed, in pioneering studies, survival was only obtained in high-density systems [23]. In later attempts, synapses did not achieve a mature state [22]. Sometimes, loss of order was observed when neurons gained

excitability [24]. When synapses were observed [27], neuronal excitability was altered as shown by the depolarized value of the resting potentials and by the firing patterns showing a single action potential. Moreover, survival was limited to less than 10 days: these neurons did not live beyond the critical survival step often described in low-density cultures [18].

The present work describes an original protocol for controlling neuronal growth on solid substrates allowing us to obtain mature and stable neuronal networks of controlled architecture that survive for weeks *in vitro*. Its success is based on (1) the use of poly-lysine instead of an aminosilane as the permissive molecule and (2) the improvement of low-density culture conditions in a defined medium in order to observe spontaneous activity and mature synapses up to 5 weeks *in vitro*. Using rat hippocampal neurons, we designed a wide variety of neuronal networks which maintain their spatial structure up to one month. The neuronal physiology remains intact for several weeks *in vitro*. Patch clamp recordings show that neuronal excitability is similar to the one observed in slices. Immunocytochemistry and electrophysiology reveal that both excitatory and inhibitory neurons form functional synapses. Characterization of neuronal connectivity with a double patch clamp approach demonstrates that connectivity is constrained by the geometry, since neurons preferentially form synapses to their first neighboring neurons. Whole cell and cell-attached recordings and calcium imaging have shown that small networks express spontaneous collective activity in a reproducible manner. Finally, we proved that our lithographic protocol could be coupled to multi electrode array (MEA) technology allowing future recording and stimulation of single neurons forming an interconnected network at a fixed location over days or weeks *in vitro*.

We have, therefore, designed a new model to study the evolution over several weeks of isolated neuronal networks that allows knowledge of the functional architecture, including the total number of interconnected neurons, the number and position of inhibitory cells and the probability of connectivity between pairs in an isolated neuronal network.

Materials and Methods

Cell Culture

Pyramidal neurons from rat hippocampus were grown on the substrates according to the protocol derived from Goslin and Banker [18]. Patterned coverslips (see below) were incubated for 5 days in neuron-plating medium containing 10% horse serum (Invitrogen, Carlsbad, Calif., USA). Hippocampi from E18 rats' embryos were dissociated chemically (0.25% trypsin, 20 min) and mechanically using fire-polished Pasteur pipettes. Neurons plated on the patterned substrates (densities ranging from 1,000 to 10,000 cells/cm²) were maintained in a 5% CO₂ atmosphere at 37°C. After 4 h, the neuron-plating medium was

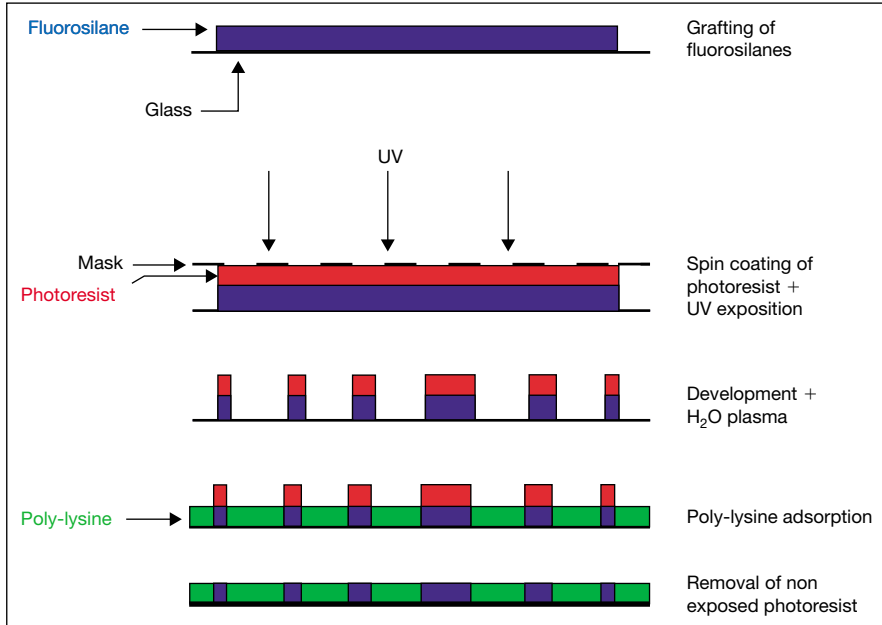


Fig. 1. Steps of the photolithography protocol. A glass coverslip (continuous black line) is coated with domains of fluorosilane molecules (blue) and with regions of poly-lysine (green) according to the pattern designed on the mask (dotted black line), using UV exposure of a spin-coated photoresist (red) (see Methods).

replaced by a serum-free maintenance medium (NMM) and a feeding layer of glial cells was added to each dish. The proliferation of glial cells in the culture was stopped by AraC after 2 days (1 μ g/ml, Sigma, St Louis, Mo., USA).

Photolithography

Each step of the protocol is presented in figure 1 and summarized in table 1. The equipment needed is listed in table 1 and some are shown in figure 2.

The coverslips placed in a ceramic rack were first cleaned in toluene in an ultrasonic bath for 10 min and dried using nitrogen. Final surface preparation before silanization could be achieved by either using a water plasma chamber (see below and figure 2a, b) used at its maximum power for 5 min or with nitric acid overnight and thorough rinsing.

The cleaned coverslips were then coated with hydrophobic fluorosilane $C_8H_4Cl_3F_{13}Si$ (Roth, France) in water-free dichloromethane and n-decane for half an hour at 4°C. Traces of water were carefully avoided to prevent bulk polymerization of the silane. Silane solutions were handled in a homemade chamber filled with argon gas. After rinsing in chloroform, the silanized surfaces were perfectly hydrophobic, which could be checked using drops of water or glycerol.

The silanized surfaces were spin-coated (fig. 2c, spin coater EC101DT (Headway Research, Garland, Tex., USA) with a positive photoresist (Shipley microposit S1813, USA).

Table 1. Lithography protocol

Equipments

Laminar flow hood, ultrasonic bath, water plasma etcher, spin coater, nitrogen gun, coverslip ceramic rack, hotplate, UV lamp, low vacuum chamber, temperature-controlled bath, masks.

Disposable

Toluene, nitric acid, bi-distilled water, fluorosilane $C_8H_4Cl_3F_{13}Si$ (Roth, France), poly-lysine (Sigma P2636), photoresist (Shipley, Microposit S1813), developer (Shipley, Microposit MF 321 Developer) and spectroscopic grade solvents: acetone, chloroform, water-free decane and dichloromethane.

Protocol

1. Clean twelve coverslips placed on a ceramic rack in toluene + ultrasonic bath 15 min, dry with N_2 .
 2. Clean with water plasma 2×5 min at maximum power or with HNO_3 overnight (in this case, rinse with a large amount of bi-distilled water (for e.g., 6×30 min) and dry with N_2).
 3. 5 min hotplate $115^\circ C$ + 10 min cooling down in the laminar flow hood flux.
 4. Grafting of the silane: fluorosilane 1 ml + 100 ml decane + 50 ml CH_2Cl_2 , under Ar, 30 min at $4^\circ C$.
 5. Rinse $2 \times$ in $CHCl_3$ (5 min in sound bath), dry with N_2 (should be completely nonwetting: hardly a droplet remains on the coverslip before drying).
 6. Spin coating of photoresist 30 s, 5,000 rpm (put drop by drop, remaining at 1 mm from edges, wait about 10 s before spin coating). Softbake: hotplate $115^\circ C$, 60 s (an Al thick sheet in close contact with hotplate).
 7. UV exposure: coverslip, photoresist face up + mask with Cr face down. Press, UV 30 s. Get back the mask, store mask with Cr face up.
 8. Developing (80 ml developer + 400 ml H_2O), $T = 20^\circ C$, 30 s. Rinse in H_2O , dry N_2 .
 9. Cold plasma: open chamber, put coverslips with the photoresist-coated face towards the magnetron. Pump down, open H_2O ($p = 0.8$ Torr). Turn on the plasma (30 s, 140 V). Turn off, close H_2O , pump, vent, open. Store chamber under vacuum.
 10. Sterile hood: coverslips in PD, sterilize with UV (254 nm) 20 min.
 11. Poly-lysine 1 mg/ml in borate buffer, filtered 0.22 μm , overnight. Rinse 2×2 h in H_2O ; transfer coverslips, 20 min in 130 ml H_2O .
 12. Dry coverslips with N_2 . Rinse $3 \times$ in acetone (5 min in ultrasonic bath). Dry coverslips with N_2 . Rinse $2 \times$ sterile H_2O . Dry coverslips with N_2 .
 13. Transfer the coverslips in PD in sterile hood. 3 ml neuron plating medium/PD; incubator.
-

This photoresist could be easily illuminated with standard hand UV lamp at 365 nm. Each coverslip was then pressed against a mask in a small chamber. We built a small low vacuum chamber consisting in two thin mylar sheets attached to circular mounts between which the substrate and the mask could be placed (fig. 2d). It was exposed to UV light for 30 s by placing the UV lamp on the top of the chamber: the close contact brought by the vacuum chamber prevented the need to use any collimation optics.

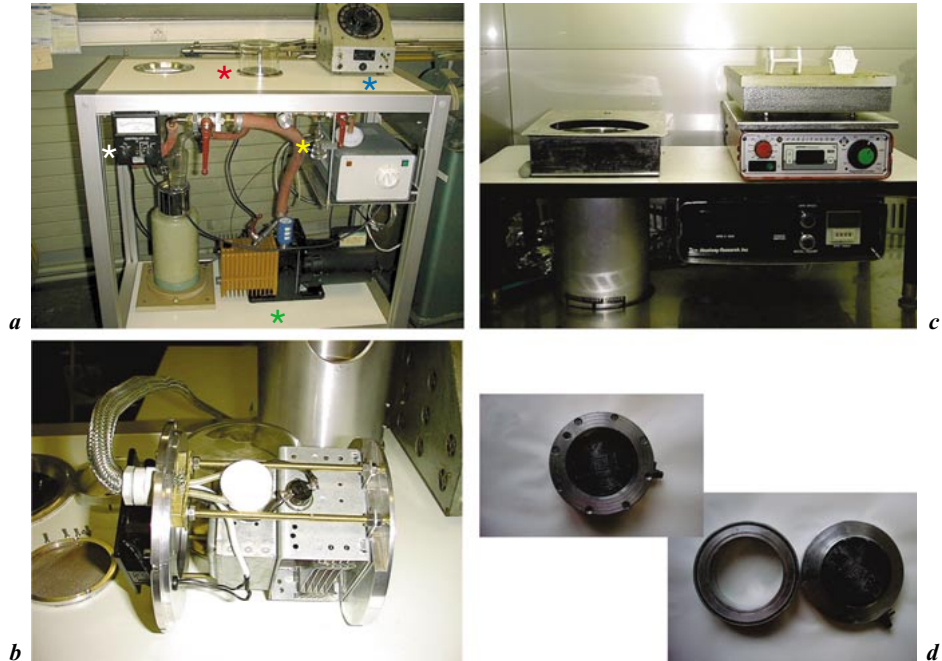


Fig. 2. Equipments for lithography. **a** and **b** The home made plasma etcher. **a** Red star: vacuum chamber; blue star: rheostat; green star: vacuum pump; yellow star: water flask and control valve; white star: vacuum controller. **b** The magnetron head, which is placed on top of the vacuum chamber. A fan was added for cooling. **c** The spincoater, the hot plate and the ceramic racks for the coverslips. **d** The small (10 cm diameter) low vacuum chamber made of two mylar sheets in which the mask is pressed against the substrate.

Incubation in a development bath (Shipley, Microposit MF 321 Developer) removed the exposed photoresist. The developer was placed in a temperature-controlled bath at 20°C to obtain repeatable duration of development. This duration was adjusted carefully to get the best resolution of the smaller details of the patterns, controlled optically after this step. After developing, the substrate was immediately rinsed in a large amount of water.

The fluorosilane layer (no longer protected by the photoresist) was removed with H₂O plasma (see below and fig. 2a, b). The substrates were placed in the vacuum chamber facing the magnetron source. Water pressure in the chamber was always fixed at 0.8 Torr. Duration and power of the water plasma (controlled by the voltage applied to the magnetron tube) were adjusted by getting the best removal of the silane layer without destroying the regions where the photoresist was not exposed. This was also checked optically with a microscope.

The glass surface was then coated with poly-D-lysine (Sigma P2636, 1 mg/ml overnight). The next day, unexposed photoresist was washed out with acetone, three times for 5 min in the ultrasonic bath. This method of removal of the photoresist was found to be totally safe for the poly-lysine coating. We chose not to use the Shipley removal solution the use of which leads to degradations of the poly-lysine layer.

To optimize our protocol, several geometrical parameters have been tested. Survival was enhanced with large poly-lysine domains (typically 80–100 μm wide) in comparison with smaller ones (e.g., 40 μm wide or less). Connecting lines of width 2–5 μm resulted in the best neurite guidance while preventing the attachment of cell bodies. Masks for lithography were easily prepared in the laboratory (see below).

Cool Water Plasma Etcher

Cool water plasma etchers are sold by different firms but can also be built in the lab at reduced cost. Our setup (fig. 2) consists of a small (10 cm in diameter and in height) low vacuum chamber in plexiglass. Vacuum is obtained with a standard mechanical pump with the appropriate tubings and measured with a Pirani gauge. A valve connected to a bi-distilled water flask allows careful adjustment of the water pressure to 0.8 Torr. The magnetron source was removed from a commercial microwave oven and centered on top of the vacuum chamber. It was powered through a rheostat allowing variation of the voltage at the magnetron source and the power of the plasma itself. By varying the voltage of the power supply, the plasma color changes from violet to orange and finally to white and accordingly its temperature and energy density. We chose the proper voltage for etching during the protocol of lithography as explained above, whereas for surface cleaning the maximum voltage was used, taking care of the rise of temperature in the chamber (no more than 5 min of etching was used in this condition).

Mask Preparation

Masks can also be purchased from several companies. It can, however, be convenient to prepare custom masks in the lab, especially if uncommon patterns need to be prepared. Low-resolution masks ($>100 \mu\text{m}$) can be directly printed onto a transparency. Intermediate resolution masks (20–100 μm) can be obtained by taking a good quality photograph of a laser print, with a reduction factor of about 10. Both the photograph negative and the transparency can be used directly and are of extremely low cost. Higher resolution masks can be obtained as described below by projection with a microscope and will require the use of a thermal evaporator to deposit a thin metallic coating such as chromium. The details of the protocol are also indicated in table 2.

In this case, any desired pattern is first drawn using standard graphics software and printed on high-quality paper using a high-resolution printer. A photograph of the printed pattern is used as a first reduction. Typically a reduction by a factor of 10 is achieved. The negative provided by the photograph is then reduced to its final size by projecting it about 100 times onto a photoresist-coated coverslip (fig. 3a). The photograph negative which was previously converted in a metallic mask by standard lithographic methods (see table 2), was placed at the position of the field diaphragm of the fluorescence light path in an Axiovert 135 inverted Zeiss microscope (fig. 3a). A glass slide coated with photoresist was placed at the focal plane of a 20X Plan Neofluar Zeiss objective. This corresponds to a second reduction by a factor of about 13, according to the value of the tube lens on the fluorescence path. A highly homogeneous illumination of the mask was achieved in order to obtain the proper illumination of the substrate coated with photoresist. By the transient opening of the shutter and appropriate displacements of a motorized stage, the mask is then printed several times on the glass slide. Duration of the illumination was carefully adjusted. After a standard metallization procedure with chromium, we obtained typically a hundred chromium patterns on a coverslip with a final size for each pattern of 0.8–1.2 mm and with a 2–4 μm resolution (fig. 3b).

Table 2. Protocol to design masks: metallic masks

Equipments

Laminar flow hood, ultrasonic bath, thermal evaporator, spin coater, nitrogen gun, coverslip ceramic rack, hotplate, UV lamp, low vacuum chamber, temperature-controlled bath.

Disposable

Toluene, sulfuric acid, H₂O₂, bi-distilled water, photoresist (Shipley, Microposit S1813), developer (Shipley, Microposit MF 321), HMDS (Sigma) and spectroscopic grade solvents: acetone, toluene.

Protocol

A: Preparation of photoresist-coated glass coverslips

1. Wash with toluene + ultrasonic bath 15 min. Dry with N₂.
2. Wash with the following acid solution: 40 ml H₂O₂ + 80 ml H₂SO₄ for 15 min. Rinse with H₂O 10× in 150 ml. Dry with N₂. Place on the hotplate at 115°C for 5 min and let it cool down 10 min.
3. Spin-coat with HMDS 30 s at 5,000 rpm.
4. Spin-coat with photoresist 30 s at 5,000 rpm. Hardbake 60 s at 115°C on the hotplate.

B: Projection of the photograph negative on the photoresist-coated glass coverslips

1. Place the photograph negative at the location of the field diaphragm. Place the photoresist-coated glass coverslips at the focus of the objective 20×.
2. Print several times (up to 100) the pattern on the substrate by appropriate opening and closing of the shutter and displacement of the microscope stage, taking care to keep the substrate in focus.
3. Developer (80 ml developer + 400 ml H₂O, T = 20°C) for 30 s. Rinse with H₂O, dry with N₂.
4. Metallization (see below).
5. Reproduction to obtain several copies of the mask (see below).

C: Reproduction

1. Place the coverslip in the low vacuum chamber in contact with the metallic mask. Expose to UV 30 s. Develop 30 s. Rinse with H₂O, dry with N₂.
2. Metallize.

D: Metallization

1. Wash with soft acid (100 ml H₂O + 20 ml H₂O₂ + 40 ml H₂SO₄) for 5 min. Rinse with H₂O 10× in 150 ml H₂O. Dry with N₂.
 2. Place the coverslip in the thermal evaporator. Pump down to P ~ 510⁻⁶ Torr. Slowly evaporate chromium (by step of 0.2 nm) up to 50–60 nm.
 3. Rinse with acetone and ultrasonic bath for 2 min.
-

Lithography on MEAs

MEAs without lid were bought from Multichannels System (<http://www.multichannelsystems.com>). We used arrays of electrodes (diameter 30 μm) separated by 200 μm (fig. 4a, b). Details of the protocol are given in table 3. To protect the electrodes, MEA were not cleaned with acids but with organic solvents: chloroform and toluene each two times for 15 min in an ultrasonic bath. Final cleaning was achieved in the water plasma etcher for 2 min at low power.

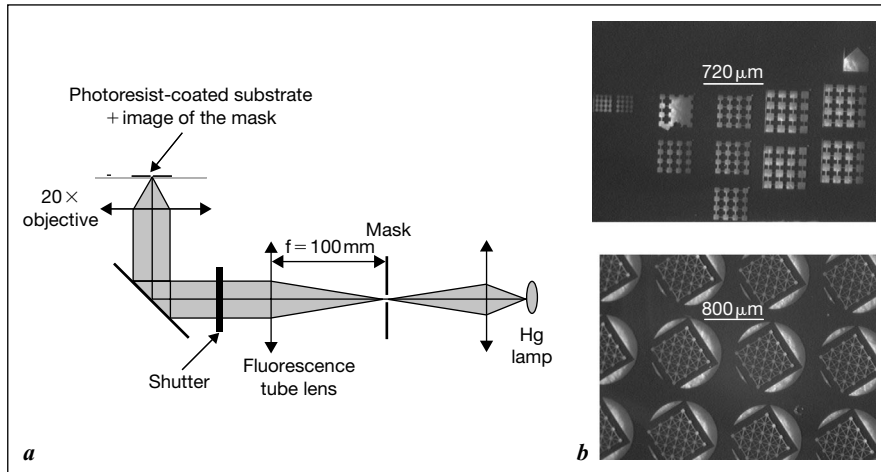


Fig. 3. Construction of masks. **a** Optical setup allowing to project, onto a photoresist-coated glass slide placed at the focal plane of the objective, an intermediate metallic mask obtained by reproduction of a negative provided by the photograph of the initial laser print. **b** Examples of masks obtained in the lab. Each pattern has a total size of about 1 mm with 2–4 μm of resolution and is reproduced about 100 times on the coverslips.

At this stage, integrity of the electrodes was checked optically and by measurement of their impedance (see below). Immediately after cleaning, MEAs were coated with fluorosilane as described for glass coverslips (fig. 1). Fluorosilane-coated MEAs were then placed on a chuck adapted to a large mount in the spin coater and coated with the photoresist (fig. 1).

Illumination of the photoresist-coated MEA was not achieved by placing the mask in contact with the substrate as in figure 1 for glass coverslips: instead it has to be aligned precisely onto the network of electrodes. Masks were, therefore, projected and aligned with an upright Olympus BX51 microscope as follows (fig. 4). An intermediate mask was designed as described above using a laser printer and a photograph of the print and further metallized with chromium. Its dimensions were calculated to match exactly the dimensions of the MEA after projection with the microscope. The mask was placed at the location of the field diaphragm of the fluorescence illumination path, which is easily accessible on this microscope. When illuminated with the mercury lamp of the fluorescence light path, it was imaged exactly on the MEA, which was placed at the focus of the microscope objective (fig. 4). The mask was fixed in this setup and MEA were displaced with the microscope stage to be perfectly aligned on the array of electrodes (fig. 4). A blue filter was added on the fluorescence light pathway during the alignment. For convenience, we chose an objective, which allows projecting in a single step the mask onto the whole MEA (the total field is about 1.5 mm), with a resolution sufficient to print the lines and provide a highly homogeneous illumination of the field of view. As the focal length of the lens on the fluorescence path is $f_f = 46$ mm in this microscope and since the focal length of an infinity-corrected objective of magnification G used with a tube lens f_i (165 mm for a Zeiss objective and 180 mm for an Olympus one) is f_i/G , the mask is, therefore, projected with a factor of reduction of $(f_i/f_f) \cdot G$. Using a Zeiss 10X, ON. 0.5, Fluor

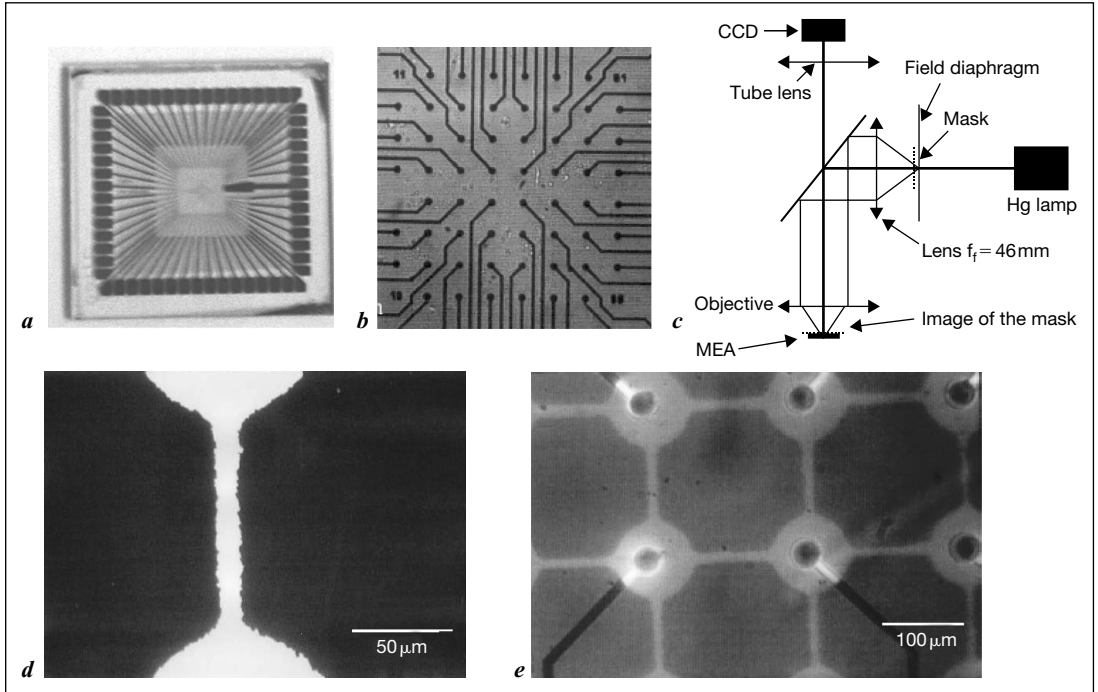


Fig. 4. Multi-electrode arrays from MultiChannels Systems. **a** View of the whole substrate (5×5 cm) with the electrodes at the center and the electrical contacts on the sides. **b** Detail of the electrodes at the center of the MEA substrate. Electrodes (diameter $30 \mu\text{m}$) are separated by $200 \mu\text{m}$. **c** Optical setup used to project the mask onto the MEA. See text for details. **d** Detail of the lines printed in the photoresist showing that their width is less than $10 \mu\text{m}$ as expected. **e** Image showing that the projected mask can be aligned exactly on the network of electrodes.

objective which provides a factor of reduction of 2.78 in this setup, a metallic mask made of circular domains of $200 \mu\text{m}$ in diameter and lines of width of about $25 \mu\text{m}$ was projected at once on the whole MEA. The neutral density filters placed on the fluorescence light path were used to adjust the illumination time to a few seconds. The final dimension of the circular domains was then about $70 \mu\text{m}$ and the width of the lines less than $10 \mu\text{m}$ (fig. 4).

After projection, the exposed photoresist was removed with the developer (fig. 1) and the silane layer below it with the water plasma etcher used at low power in the condition described above. After deposition of poly-lysine at 1 mg/ml , unexposed photoresist was removed with acetone. At this stage, a lid consisting of a Petri dish in which a 1×1 cm square hole was drilled in the center was attached to the MEA using a sterilized ultravacuum grease (Dow Corning) which was easily cleaned for subsequent use of the MEA and which was fully compatible with long-term survival of the cells in culture. Let us note that the use of paraffin is not recommended since the traces remaining after thorough cleaning were enough to prevent the proper polymerization and anchoring of the fluorosilane layer. At this step, the substrate was ready for plating.

Table 3. Coupling of lithography on MEAs: Coating MEA with adhesive pattern

Equipments

Laminar flow hood, ultrasonic bath, water plasma etcher, spin coater, nitrogen gun, coverslip ceramic rack, hotplate, UV lamp, low vacuum chamber, temperature-controlled bath, masks.

Disposable

Toluene, nitric acid, bi-distilled water, fluoro-silane $C_8H_4Cl_3F_{13}Si$ (Roth), poly-lysine (Sigma P2636), photoresist (Shipley, Microposit S1813), developer (Shipley, Microposit MF 321 Developer) and spectroscopic grade solvents: acetone, chloroform, water-free decane and dichloromethane.

Protocol

1. Clean MEA placed on a ceramic rack $2\times$ in toluene + ultrasonic bath 15 min, dry with N_2 . Clean $2\times$ in chloroform + ultrasonic bath 15 min, dry with N_2 . Final wash in plasma etcher for 2 min at low power. Place 5 min hotplate $115^\circ C$ + 10 min cooling down in the laminar flow hood flux.
 2. Grafting of the silane: fluoro-silane 1 ml + 100 ml decane + 50 ml CH_2Cl_2 , under Ar, 30 min at $4^\circ C$. Rinse $2\times$ in $CHCl_3$ (5 min in sound bath), dry with N_2 .
 3. Spin coating of photoresist 30 s, 5,000 rpm (put drop by drop, remaining at 1 mm from edges, wait about 10 s before spin coating). Softbake: hotplate $115^\circ C$, 60 s.
 4. Place the metallic mask at the location of the field diaphragm. Place the photoresist-coated MEA at the focus of the objective $10\times$. With dim white light and blue filtered fluorescence light, align the MEA onto the mask.
 5. Print the pattern on the MEA.
 6. Developing (80 ml Developer + 400 ml H_2O), $T = 20^\circ C$, 30 s. Rinse in H_2O , dry N_2 .
 7. Cold plasma: open chamber, put MEA facing towards the magnetron. Pump down, open H_2O ($p = 0.8$ Torr). Turn on the plasma (30 s, 140 V). Turn off, close H_2O , pump, vent, open. Store chamber under vacuum.
 8. Sterile hood: sterilize with UV (254 nm) 20 min.
 9. Poly-lysine 1 mg/ml in Borate Buffer, filtered 0.22 μm , overnight. Rinse $2\times$ 2 h in H_2O ; transfer in 130 ml H_2O .
 10. Dry MEA with N_2 . Rinse $3\times$ in acetone (5 min in ultrasonic bath). Dry with N_2 . Rinse $2\times$ in sterile H_2O . Dry with N_2 .
 11. Fix to the MEA with sterile high vacuum grease a Petri dish with a square hole. Add 3 ml neuron plating medium/PD; incubator.
-

To control the effect of the surface coatings on the electrode's electrical properties, we measured their impedance at each step. It was characterized over a large frequency band (1 Hz–100 kHz). The MEA was immersed in a solution of NaCl at 0.5 M. A voltage generator applied 100 mV between an Ag/AgCl electrode dropped in the NaCl solution and a 1 M Ω resistance in serial with the MEA to limit the current injected. The module of the MEA impedance was estimated by measuring the voltage drop across the resistance.

Time Lapse

In order to follow the growth of many neurons over several weeks, we built with the help of Emmanuel Jover (IPCB, Strasbourg) an incubation chamber, regulated in temperature

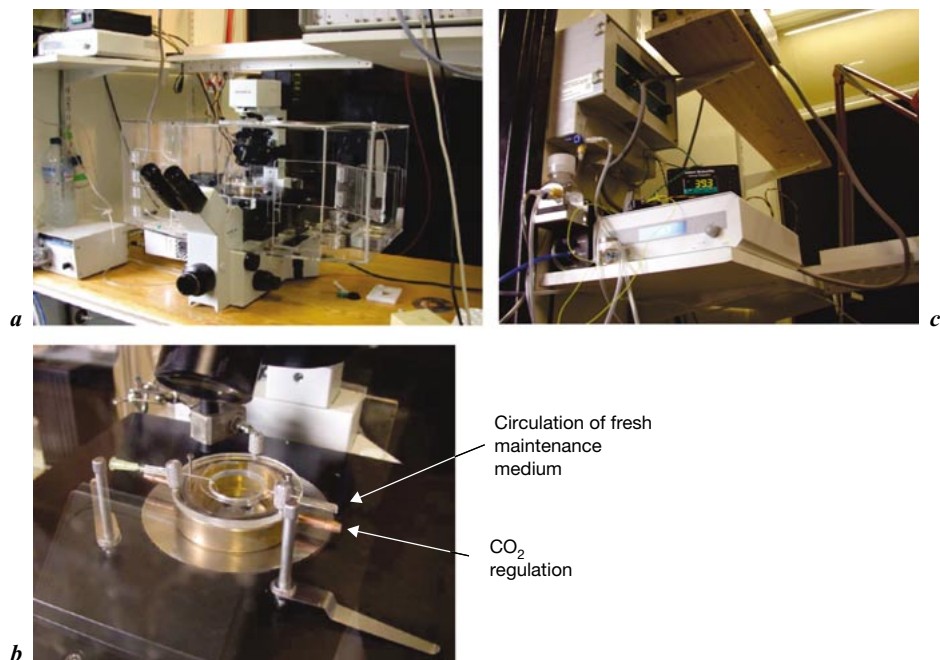


Fig. 5. Time lapse microscopy. **a** A homemade regulation of the CO₂ concentration has been added to a temperature-controlled chamber in plexiglass built on an inverted Olympus microscope with the Till Photonics acquisition system. **b** The CO₂ regulation is only achieved in a small chamber where the Petri dish is placed. **c** The CO₂ regulation system with an electronically controlled valve.

(37°C) and in CO₂ concentration (5%), and containing the sample stage of an Olympus inverted microscope (fig. 5). We observed in DIC the growth of the cultures in NMM fed by a glial cell layer from day 1 to 10 after plating. An image was acquired every 20 min.

Electrophysiological Recordings

Cell-attached and whole cell patch clamp recordings were obtained at room temperature from 1- to 4-week-old cells. All recordings were performed using Axopatch 200B (Axon Instruments, Foster City, Calif., USA). Patch pipettes were made of borosilicate tubes (Clarks, UK) and had a resistance of 3–4 MΩ when filled with the standard pipette solution. In cell-attached recordings, a 5 mV pulse was regularly applied to insure that the perforation of the neuronal membrane had not occurred. During whole cell recordings, to monitor the recording characteristics, leak resistance was measured periodically and ranged between 250 MΩ and 1 GΩ for a given cell. Leak current monitored in voltage clamp recordings ranged from 10 to 200 pA. Cells older than 3 weeks with larger surfaces could sometimes not be clamped in voltage mode and would fire a spike on the edge of the excitatory post synaptic currents (EPSC) in this configuration. We discarded these cells for our analysis of

synaptic properties. Collection of data was interrupted if the recording showed a significant change in leak resistance. Fast and slow capacitance and series resistance compensation were performed in the whole cell mode. Series resistance in whole cell configuration was less than 10–12 M Ω , and was compensated up to 60%. Data were acquired at 5 kHz in real time with an Axon Digidata 1320A (Axon Instruments).

Recording Solutions

The bath solution contained in mM 145 NaCl/3 KCl/3 CaCl₂/1 MgCl₂/10 Glucose/10 HEPES/pH = 7.25 and its osmolarity was adjusted to 315 mOsm. The pipette solution contained in mM 9 NaCl/136.5 KGlu/17.5 KCl/0.5 CaCl₂/1 MgCl₂/10 HEPES/0.2 EGTA/pH = 7.25 and its osmolarity was equal to 310 mOsm. The bath solution was perfused locally at 0.5–1 ml/min with a microperfusion tube inlet and outlet from a peristaltic pump. All experiments were performed at room temperature (22–25°C).

Calcium Imaging

Cultures were loaded with 5 μ M of the membrane-permeant acetoxymethyl ester of Fura-2 AM (ref. F-1201, Molecular Probes) for 15 min at room temperature and then rinsed for 30 min. A 100 W xenon lamp filtered at 380 nm ensured excitation of the probe and emission occurred above 510 nm. 8 \times 8 binned images obtained at 20 Hz with a CCD (CoolSnap HQ, Roper Scientific, Duluth, Ga., USA) were stored and analyzed using Metamorph in order to measure the fluorescence intensity variation in a cell body. Each spike in a Fura-2 AM-loaded neuron leads to a large calcium entry associated with a decrease of the fluorescence emission [39]. The variations of fluorescence intensity in the soma reflect the occurrence of spikes with the time resolution of our acquisition system (50 ms). The concentration of Fura-2 in the soma was estimated to be of the order of about 50 μ M.

Multiple Calcium Imaging Trials

By reloading the cells placed in the time lapse setup with Fura-AM used at low concentration (1 μ M, 15 min), we were able to record the variation of the intracellular calcium concentration over several days. The noise associated with the metabolism of the probe was small enough to perform spike-timing analysis on each trial.

Results

Photolithography Protocol

The protocol of photolithography (see Methods, table 1 and fig. 1) is based on an adhesion contrast between a hydrophobic monolayer made of fluorosilane molecules and hydrophilic poly-lysine patterns confining the cell bodies to large domains (\sim 100 μ m) and the growth of neurites to thin lines (2–5 μ m wide and 100 μ m long). The density of neurons was adjusted so that on average a single neuron was located on each poly-lysine domain (see images of various networks on fig. 6).

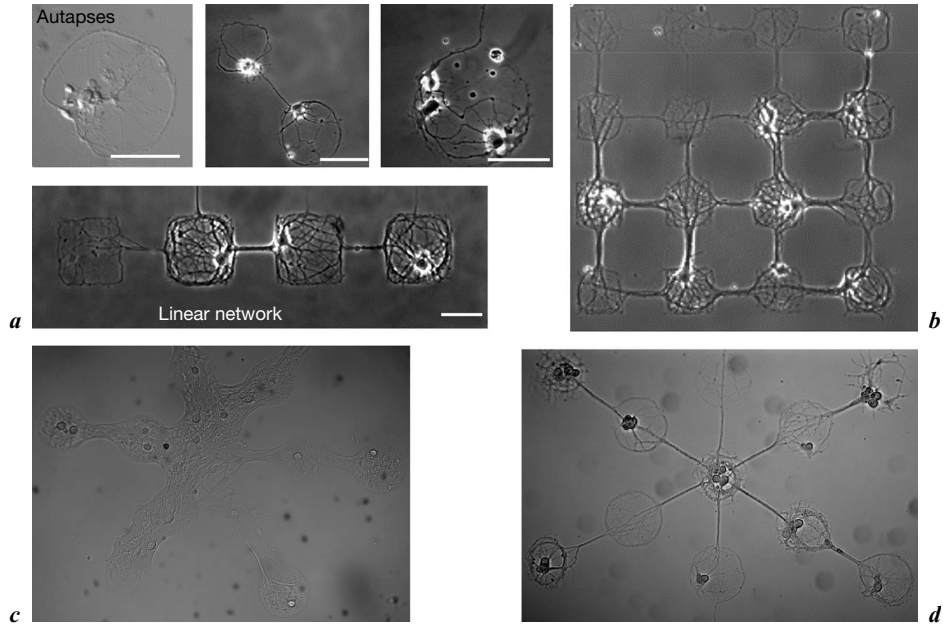


Fig. 6. Images of the cells grown on the chemical patterns. **a** Images of neural networks of controlled architecture when glia proliferation is inhibited, with diverse geometry: autapse (top left); pairs (top middle and right); linear network (bottom). **b** Matrix (4×4) network. **c** Images of neural networks of controlled architecture when glia proliferation is not inhibited (star pattern). The patterns are then less defined because glial cells covered the fluorosilane layer. Somas are then allowed to move from one domain to the other. **d** Images of neural networks of controlled architecture when glia proliferation is inhibited (star pattern). Cell bodies of neurons are restricted to squares or disks of $80 \mu\text{m}$ and neurites to lines ($80 \mu\text{m}$ length, $2\text{--}4 \mu\text{m}$ wide). Square and disk diameters are $80 \mu\text{m}$ for each figure. Scale bar = $50 \mu\text{m}$.

Our protocol uses standard techniques of photolithography to establish the adhesion contrast on glass coverslips (fig. 1). It requires minimal equipment (see fig. 2): mainly a sterile laminar flow hood (to avoid dust on the substrates), a spin coater (to cover the glass coverslips with a photosensitive resist) and a cool water plasma etcher (to remove the covalently bound silane monolayer and to clean the surface prior to poly-lysine adsorption). Some of the equipments can be homemade as for example the plasma etcher or the UV illumination chamber (see fig. 2). High-resolution masks were also made in the laboratory with a thermal evaporator (see examples on fig. 3), but they can also be obtained commercially. Low-resolution masks (smaller details larger than $20 \mu\text{m}$) can be designed at no cost with a good ink-jet or laser printer. The lithography protocol

requires only a few hours once a week for each culture. It is very reproducible and easy to learn since none of the steps are particularly difficult.

Primary cultures were obtained from rat embryo hippocampus following the classical Banker protocol [17]. We noted that the long-term survival of the cells was dramatically improved if the glial cell feeding layer was used prior to confluence. The success of our lithography protocol in comparison with the previous ones [22–24, 27, 28] lies in the combined use of (1) a culture protocol for nonmitotic cells, (2) without serum and (3) a standard adhesion substrate, poly-lysine to enhance cell adhesion. Indeed the protocol does not operate neither if the serum is present in the extracellular maintenance medium nor if glial cell division is not inhibited with AraC (see fig. 6): the pattern is lost with time since mitotic cells proliferate rapidly on fluorosilane domains (compare fig. 6c, d), and neurons alone in the presence of serum are also invading the hydrophobic regions slowly with time. Most of previous works had estimated that the use of poly-lysine would be delicate in a protocol of photolithography. Since poly-lysine is an excellent substrate for neuron growth in culture, we have adapted standard lithography protocols to use it safely.

Control of Neuronal Position in Different Architecture

Poly-lysine, a polymer of basic amino acids, is commonly used to promote cell adhesion. Patterning by lithography was thought to be difficult because of its size and the resulting thickness of the layer on glass [24]. Our strategy to pattern poly-lysine (see Methods and fig. 1) relies on the use of H₂O plasma to clean the surface prior to poly-lysine deposit and on the removal of the unexposed photoresist with acetone which does not degrade the coated poly-lysine. We obtained micron scale patterns of poly-lysine which target cellular bodies and guide neurites to form spatially directed neuronal networks (fig. 1 and 6).

A wide diversity of patterns has been designed to form autapses, linear networks, matrices and stars (some shown in fig. 6). In the patterns (fig. 6), neuronal soma adhered to the 100 μm -wide spots of poly-lysine (square or disc) but not to the poly-lysine lines connecting two domains because of their thinness (2–4 μm wide). Neurite elongation occurred within spots and thin lines (100 μm long). We could localize cell body adhesion and guide neuritic growth within certain geometrical conditions (see Materials and Methods). Somatic adhesion sites had to be at least ~ 60 –80 μm in diameter. The width of poly-lysine lines should be inferior to 10 μm in order to allow neurites elongation and to prevent cell body adhesion. Their length was set to ~ 100 μm to allow formation of connections. Longer distances were not favorable to

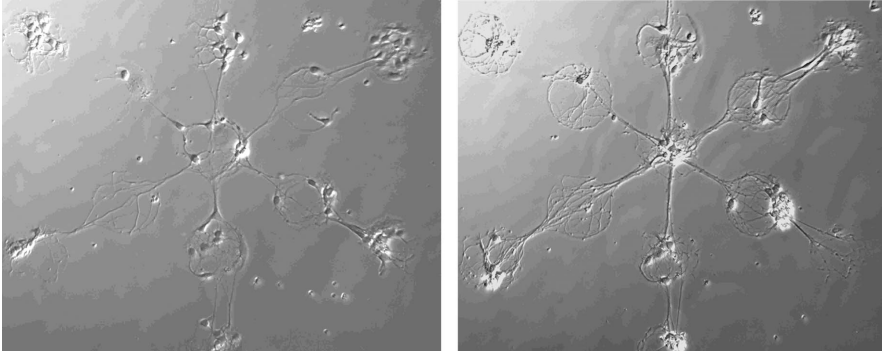


Fig. 7. Cell bodies remain on the same poly-lysine disk over time. Time lapse imaging of a neuronal network on a patterned substrate over time *in vitro*: two days after plating (left); nine days after plating (right). Images acquired over time demonstrate that growing neurites follow the chemical pattern, whereas the cell bodies remain located within the same poly-lysine domain.

maintain good neuronal survival [29], whereas shorter distances increased the probability that some neurites escape from the poly-lysine lines by ‘jumping’ directly to the next poly-lysine domains.

Adhesion, Growth and Morphology of Neurons

The number of cells per domain was determined through the plating density, thereby fluctuating from one pattern to the next. We adjusted the plating density in order to have an average of one cell per spot (see fig. 6). The guidance of the neurons by the chemical pattern was preserved in serum-free medium *in vitro* for as long as 5 weeks. During that period, neurons soma did not escape from the poly-lysine domains in which they had been trapped during the first few hours after plating. This has major advantages, with respect to standard cultures, that each neuron can be identified in a given pattern and studied over time. The neuronal morphology (fig. 6) was similar to the one observed in classical low-density cultures [18]. We studied neurons after one week *in vitro* when they always exhibit a large number of neurites (fig. 6).

Maintenance without Soma Movement over Weeks in vitro

The observation of neuronal growth on a time lapse setup (see fig. 5) allowed characterizing neuronal development over a week. Two hours after plating, cell bodies had adhered only on the large poly-lysine domains; in the first few days, their neurites grew on the thin lines connecting domains. After 5 days, somas could still move within their poly-lysine domain but remained on it. After a week, neurites had elongated over several domains without leaving the poly-lysine-covered zones (see fig. 7). At that stage, soma did not move any

more within a domain. With this new protocol, the adhesion contrast was, therefore, preserved over weeks and cell bodies were forced to keep their location (see fig. 7).

Therefore, in contrast to standard cultures, on patterned substrates the position of somas does not change during maturation *in vitro*. Even without using time lapse, a given network can be identified by the number and position of neuronal cell bodies. Therefore, it is very easy to recognize a given network within a Petri dish and follow it over weeks *in vitro* to study, for example, the evolution of interactions between constitutive neurons, or the effect of pharmacological compounds [1, 2] on neurite elongation or synapse formation.

Physiology of Neurons and Their Synapses Preserved

In order to use lithographical techniques, it was critical to show that mature neurons had a similar physiology when plated on patterned substrates and on standard substrates. Patch clamp recordings coupled to the immunodetection of synapses demonstrated the integrity of neurons in terms of (1) morphology (presence of gamma amino butyric acid (GABA)ergic and glutamatergic neurons in a proportion similar to the one measured *in vivo*, i.e., between 10 and 25%; see fig. 8c); (2) excitability (membrane resistance and firing patterns, see fig. 8a, b); (3) synapses maturation (electrophysiological characterization, immunological and pharmacological identification of α -amino-3-hydroxy-5-methyl-4-isoxazolepropionic acid, N-methyl-D-aspartate (NMDA) and GABA-A receptors; see fig. 9) and (4) occurrence of spontaneous electrical activity up to 5 weeks (see fig. 12). These results constitute an important progress and might open the way to long-term physiological studies on neuronal networks *in vitro*.

Electrophysiological Characteristics of Neurons Are Intact

Electrophysiological properties of neurons grown on patterned substrates were similar to those observed in classical ‘random’ low-density cultures. Using patch clamp (in the whole cell configuration), we evaluated and compared membrane properties and firing patterns of neurons in both systems. As shown in figure 8a, there were no differences in resistance, capacitance and time constant of the membrane between the two types of culture. In all cases, membrane resistance ranged approximately between 100 M Ω and 1 G Ω (239 ± 17 M Ω) as observed in standard cultures (217 ± 28 M Ω ; see also [30]). To evaluate cell excitability, resting potential and firing patterns were compared in standard and patterned cultures. Resting membrane potentials varied between -50 and -60 mV in both culture types (-55.6 ± 2.3 mV for standard low-density

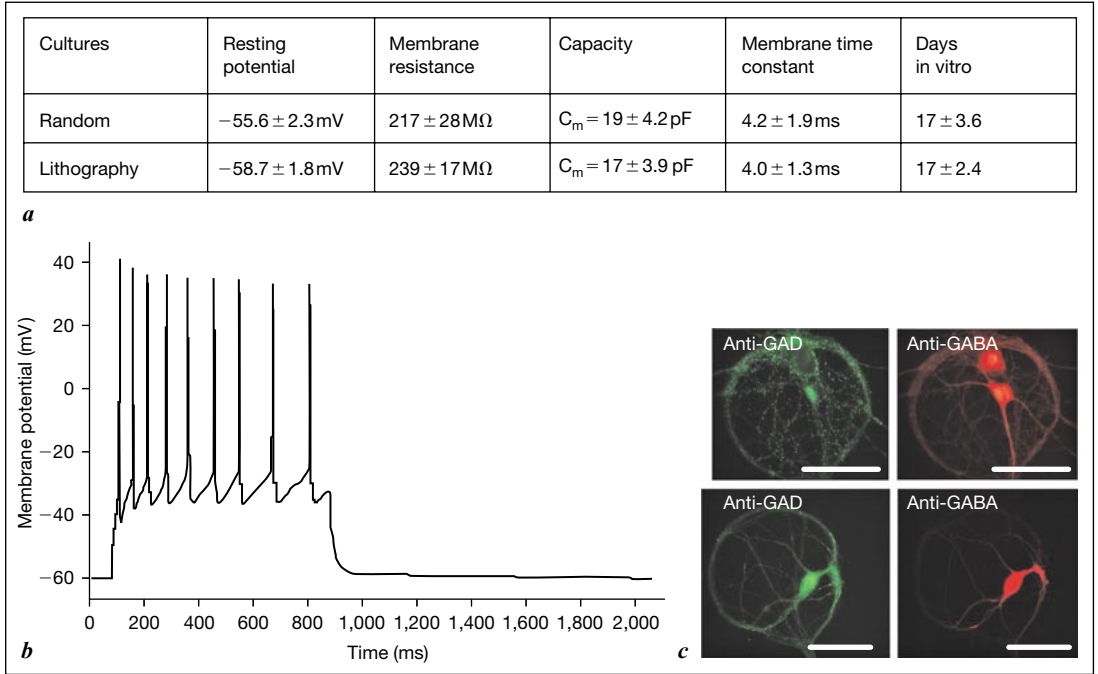


Fig. 8. Physiology of neurons grown on poly-lysine patterns is similar to the one observed in standard low density cultures. **a** Membrane biophysical properties. **b** Firing patterns observed in cultures in standard conditions as after the lithography protocol (firing patterns were obtained after a depolarizing step of 800 ms with CNQX and bicuculline added to the bath). **c** Detection of GABAergic synapses by immunocytochemistry using anti-GABA (red) and anti-GAD65 (green). Upper images: the upper neuron is glutamatergic, the lower one is GABAergic. Lower images: the neuron is GABAergic. Scale bar = 50 μ m.

cultures and -58.7 ± 1.8 mV for patterned cultures) and the firing patterns were similar (fig. 8b). In response to a 800 ms depolarizing pulse, neurons usually discharged multiple action potentials which habituate. A smaller fraction [18% for patterned cultures ($n = 52$) and 17% for classical cultures ($n = 31$)] exhibited a single spike response (*not shown*). All current-evoked action potentials disappeared after extracellular application of 0.5 mM tetrodotoxin ($n = 7$). The similarity of these results with those obtained in acute slices [31] demonstrates the integrity of the membrane and the excitability of neurons in our conditions.

Inhibitory and Excitatory Cells Are Both Present

We observed both GABAergic, identified by immunoreactivity for GABA [5], and nonGABAergic, presumably glutamatergic, neurons (fig. 8c). The patterned neuronal networks were slightly enriched in GABAergic cells [27%

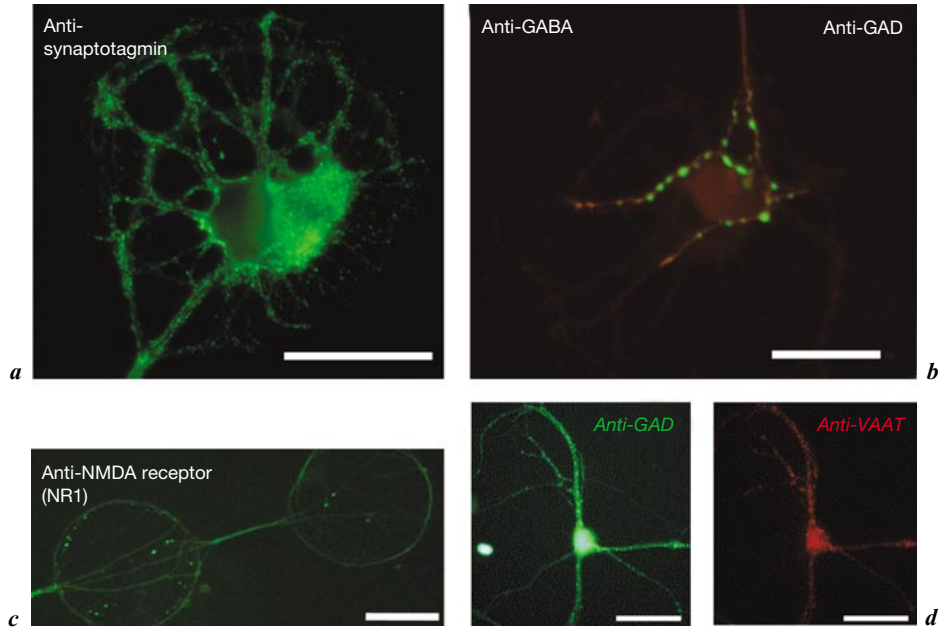


Fig. 9. Neurons form mature synapses on patterned surfaces. **a** Detection of synapses by immunocytochemistry using anti-synaptotagmin antibody (green). **b** Detection of GABAergic synapses by immunocytochemistry using anti-GABA (red) and anti-GAD 65 (green). **c** Detection of glutamatergic synapses by immunocytochemistry using anti-NMDA receptor (NR1) (green). **d** Detection of GABAergic synapses by immunocytochemistry using anti-VAAT (GABA transporter, red) and anti-GAD 65 (green).

of the overall population in patterns ($n = 432$) compared to 22% in standard cultures ($n = 513$). We conclude that both inhibitory and excitatory neurons grow on patterned networks. But do they form an interconnected neuronal network? The presence of synapses was assayed by immunostaining with antibodies against marker proteins of presynaptic specializations, synaptophysin and synaptotagmin. Immunoreactivity for each protein was distributed in clusters, corresponding presumably to synapses, spread all over the networks (see fig. 9). Moreover, we have shown evidence for functional synapses by recording spontaneous synaptic currents [32].

Neurons Form Mature Inhibitory and Excitatory Synapses

Whole cell recordings revealed spontaneous (excitatory and inhibitory) synaptic currents distinguished by their reversal potential and by specific pharmacological agents sensitivity. Inhibitory post synaptic currents were sensitive to the GABAA receptor antagonist bicuculline methiodide (1 mM) and

reversed polarity near -45 mV. Their decay time constant was 45 ± 7 ms. EPSCs were sensitive to 10 mM 6-cyano-7-nitroquinoxaline-2,3-dione, which blocks α -amino-3-hydroxy-5-methyl-4-isoxazolepropionic acid-type glutamate receptor. These currents reversed near 0 mV (1.1 ± 2.3 mV) and their decay time constant was 2.0 ± 0.7 ms. The reversion values were coherent with the ionic concentrations (see Methods) and the current kinetics with those observed in slices [33] or dissociated cultures [34, 30].

We attempted to compare qualitatively the spatial distribution of inhibitory and excitatory synapses. Immunocytochemistry for glutamate acid decarboxylase 65 (which stains cell bodies and synaptic terminals of GABAergic cells) showed that inhibitory synapses are concentrated around the cellular bodies of excitatory neurons (see fig. 9) more than on neurites (GABAergic synapses on cell bodies of GABAergic neurons cannot be identified since glutamate acid decarboxylase 65 staining is very dense in these cell bodies). On the other hand, NMDA receptor-positive synapses revealed by staining for NR1 (NMDA receptor subunit 1 common to all NMDA receptors, expressed by all neurons) were widely distributed on the neurites (fig. 9b). Both the glutamate acid decarboxylase and NR1 staining matched the labeling observed on 'mature' neurons in culture [35].

A great advantage of controlled architecture network in comparison with standard culture lies in the high probability of connections between neighbors after 2–3 weeks in vitro. We can, therefore, follow over a month the evolution of synapses formed between two identified neurons. This is a great advance in the technique of neuronal cultures, allowing in particular to follow the effect of chronically administrated pharmacological agents over the development of identified synapses [1, 2].

Orientation of Synaptic Connectivity

Since neurons form mature synapses after a week in vitro, we have evaluated whether their formation was orientated by the geometry of the pattern. As our protocol does not favor the growth of neurites versus axons in the thin poly-lysine paths and does not restrain neurites growth on the poly-lysine pattern, it was not obvious that synaptic connectivity between neurons was related to geometry. In order to evaluate the connectivity as a function of distance, we designed masks representing stars with six branches with the idea that a neuron in the center (with the largest number of neighboring neurons) should be more connected to others, while a neuron in the periphery (with less partners in a close neighborhood) might be less connected to the rest of the network.

The connectivity has been quantified between pairs of excitatory neurons in the networks from five to ten neurons between 2 and 3 weeks in vitro. With

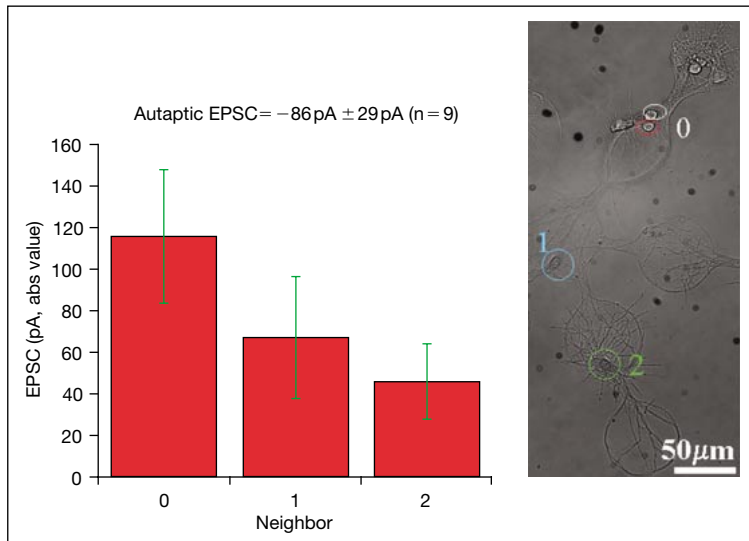


Fig. 10. Amplitude of EPSCs decreases as a function of distance between neurons in a controlled architecture network after 2–3 weeks *in vitro*. Double voltage clamp recording was performed on pairs of neurons of a network. A cell on the disk 0 was stimulated by a brief depolarizing voltage pulse. If a cell 0 forms excitatory synapses on cell 1, the stimulation of cell 0 was followed by the recording of an EPSC in cell 1 after 5–10 ms. On the histogram, EPSCs' amplitude was averaged between different pairs of neurons: for neurons on the same disk (called neighbors '0', $n = 9$), for neurons on neighboring disks (called neighbors '1', $n = 12$) and distant neurons (called neighbors '2', $n = 9$). EPSCs amplitude, which reflects approximately the number of functional glutamatergic synapses formed by one neuron on another, decreases with distance (mean EPSC amplitude for an autapse: $86\text{ pA} \pm 29\text{ pA}$).

a double patch approach, we tested if a connection existed between excitatory neurons as a function of their distance in the network by observing the occurrence of a monosynaptic response between them. A synaptic response is assumed to be monosynaptic when an EPSC occurs after a short delay (inferior to 10 ms) and has a monoexponential decrement. When a monosynaptic response was recorded, we measured also its amplitude to evaluate the efficiency of the connection (see fig. 10). The main results are the following. A glutamatergic neuron always formed synapses onto itself (homo-synapses or autapses) and on another neuron located on the same disc (hetero-synapses); the probability of monosynaptic contacts between first neighbor neurons was more than two times larger than the one of distant neurons (90 and 40% respectively, see fig. 11). The amplitude of the monosynaptic response decayed also as a function of the distance between neurons in a

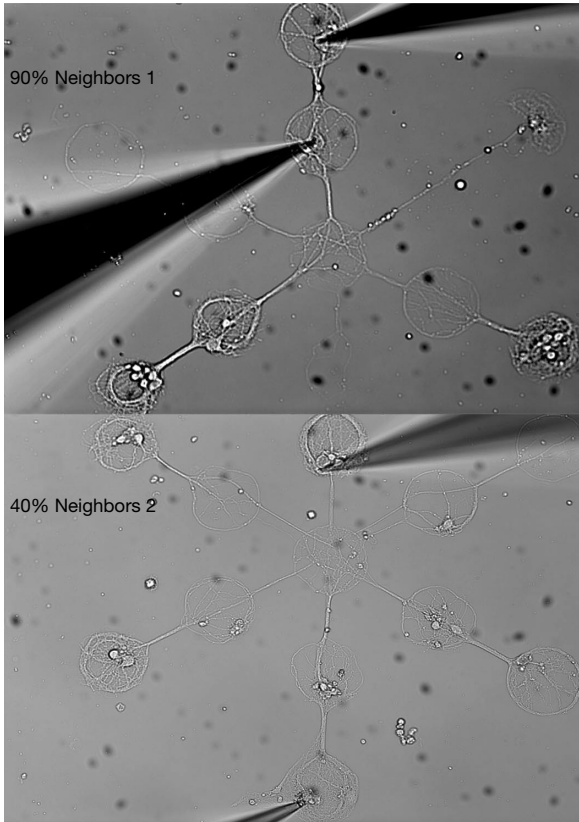


Fig. 11. Distance between neurons was associated with a probability of synaptic connections between pairs of excitatory neurons in a controlled architecture network between 2 and 3 weeks in vitro. Different types of neuron pairs are patched in the figure. Top: first neighbor. Bottom: second neighbor. The average probability of connection (quoted in the image) decreases with distance between neurons. Note that this distance does not really correspond to a physical distance, because it takes into account also the number of intermediary neurons.

network (see fig. 10 and 11): proximal neurons were forming more synapses between each other.

These observations lead to the conclusion that there is a connectivity gradient between excitatory neurons which is imposed by the geometry of a network. This is the first evidence that an architecture controlled by lithography can determine the functional structure of a network. This functional structure (which is summarized in fig. 16 in the case of our network) was defined as the total number of neurons, the presence and position of inhibitory neurons and the probability of connectivity associated to the distance between neurons. Of course, this last

information is only a statistical average. Nevertheless, it may be extremely useful for the interpretation of data and the modeling of the activity of networks.

Study of Spontaneous and Evoked Activity over Long Term

Current clamp experiments showed that tetrodotoxin sensitive spikes could be induced after 3 days *in vitro*. Spontaneous postsynaptic potentials appeared between 4 to 7 days. Cell-attached experiments showed that both the number of spontaneously active cells and their rate of discharge increased with time. After 3 weeks *in vitro*, spontaneous action potentials often appeared in bursts (fig. 12b). This bursting activity was blocked by the application of 10 mM 6-cyano-7-nitroquinoxaline-2,3-dione (*not shown*). To probe whether this spontaneous activity occurred simultaneously throughout the network, we used calcium imaging with Fura 2 AM probes (fig. 12) [16, 36–39]. Single action potential triggered an increase in intracellular calcium concentration in the soma, which causes a decrease of fluorescence intensity (with a time peak of 10–20 ms and a time decay of about 1 s). We measured fluorescence intensity over all the neurons of the network every 20 ms (fig. 12). We observed that calcium increased in all the neurons of the network during a burst of action potentials (fig. 12) suggesting that all neurons were usually active during a burst. Therefore, in patterned networks, spontaneous activity evolved with time from random isolated spikes to bursting spike formation similar to what has been seen for cortical dissociated cultures and in young slices [40, 41].

A detailed analysis of the spontaneous pattern of activation as a function of the functional architecture can be performed using calcium imaging of the electrical activity of these patterned networks. The validity of our optical method of spike identification was confirmed by simultaneous cell attached and calcium imaging recordings. More than 95% of the spikes were correctly discriminated. Figure 13 shows some examples of such an analysis. Groups of neurons whose activity was strongly correlated during the acquisition can be identified and linked to their relative position, in particular, to inhibitory neurons. We observed among others that highly synchronous subnetworks of excitatory cells correspond to close (and therefore, strongly connected) neurons on the pattern (see fig. 13d). Moreover, inhibitory neurons play a key role in defining synchronous subnetworks.

Finally, the electrical activity in these networks can be followed over long periods by optical methods with our time lapse setup. We could indeed stain neurons with Fura 2-AM repeatedly from one day to the other. Calcium imaging allows, therefore, following the evolution of electrical activity of neurons over several days.

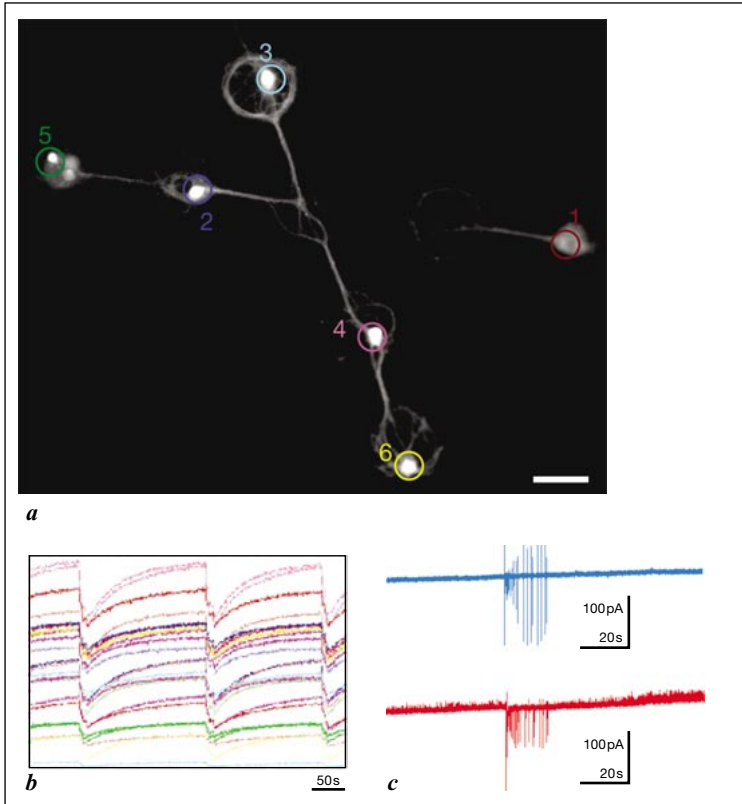


Fig. 12. Optical detection of spontaneous activity with calcium imaging. **a** Fluorescence image of a neuronal network after Fura-AM loading. The network contains 6 cells (circles). **b** Spontaneous activity estimated from calcium imaging of a network. **c** Spontaneous activity recorded from double cell attached experiments. Both calcium imaging and cell-attached recording show that spike emission is synchronous in different cells of the same network and that spontaneous activity occurs through large collective bursts separated by long silences.

Coupling to MEAs

Even if calcium imaging of activity can be used successfully, it raises, nevertheless, some difficulties, which are linked to its weak temporal resolution and to the toxicity of metabolism of the AM probes. Due to these limitations, we tried to achieve the coupling of lithography to the technology of MEAs [42, 43]. The combination of these two approaches should allow recording without toxicity and with a good temporal resolution (\sim ms) of all neurons

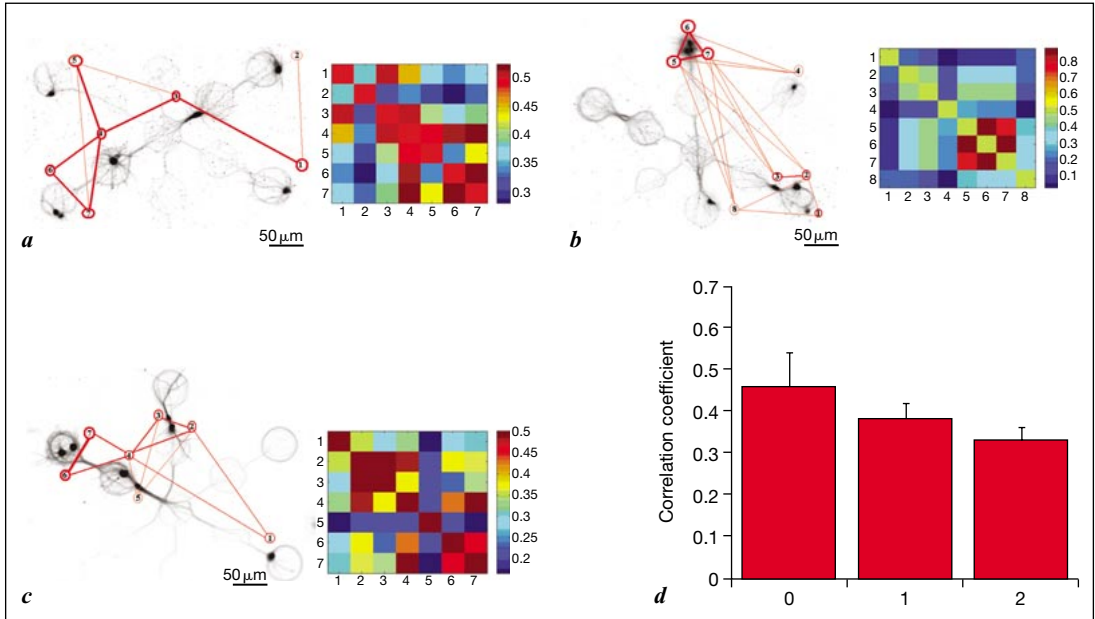


Fig. 13. Correspondence between geometry and correlation of activity in different excitatory networks with 7–8 neurons: close excitatory neurons are highly synchronized. Spike detection was estimated through calcium imaging with 50 ms time resolution and 95% efficiency. Three examples of networks in **a**, **b** and **c**. For each, negative fluorescence image of the network (left) and map of the correlation of activity (right). A red line links neurons with high correlation. The width of the red line is proportional to the degree of correlation. **d** Correspondence between distance and correlation of activity between neurons in excitatory networks. Neurons on a same disk = 0; first neighbors = 1; second neighbors = 2. Correlation of activity, as synaptic connectivity, decreases as a function of distance between neurons.

simultaneously within the same network. The electrodes of MEAs allow, moreover, stimulating the neurons selectively [44].

We have for these reasons modified our protocol so that it could be used with MEA. This mainly implied using only organic solvents instead of acids for the cleaning procedure and to find an easy way to align the mask onto the MEA in order to print the adhesive contrast.

To control the surface treatments from damaging the MEA's electrodes, we measured their impedance at each step of the protocol. Figure 14a shows the impedance of an electrode after the initial cleaning, the silanization, the plasma etching and the poly-lysine coating, respectively. Results depended slightly on

the electrodes but the main tendencies are evidenced on the figure 14. The electrodes behaved as expected as a circuit composed of a resistance and a capacitance in series. The corner frequency of the circuit was of the order of 1 kHz. The impedance at 1–10 kHz (which matters for the recording of action potentials) was of the order of several 100 k Ω . The exact value varied slightly from one electrode to the other and was very sensitive to the initial cleaning step. The silanization of the surfaces affected dramatically the impedance which rose by more than one order of magnitude. However, after the revelation of the photo-resist and removal of the silane layer below it, the impedance recovered its initial value. Final deposition of the poly-lysine had a small or negligible effect. We can, therefore, conclude that our protocol preserves the electrical properties of the electrodes. This is of major importance since their chemical nature and shape have been optimized for the proper recordings of the electrical activity. We did not investigate by electron microscopy the microscopic organization of the electrodes which consists of a hairy-like structure obtained by sputtering; but the macroscopic recordings of their impedance is a strong evidence in favor of their conserved properties.

Using our protocol, it was possible to localize selectively the neuron cell bodies onto the MEA's electrodes or close to them as shown on fig. 14c–f, which are images of the neurons grown on the MEA whose electrodes had been selectively coated by poly-lysine. They can be compared to the images shown on figure 14b, where neurones were grown on a MEA without a chemical pattern. Rapid comparison indicates clearly that the chemical pattern increased the number of electrodes having a neuron close to it. In the case of MEA coated with a chemical pattern, the number of cells per electrode could be varied depending on the density at which the culture was plated. At high density each electrode had several cells close to it, whereas at low density only a few electrodes were close to a neuron. Optimization of the plating density provided, therefore, a situation at which statistically about 75% of the electrodes had a single neuron in their vicinity. For optimal recordings, it is usually admitted indeed that neuron cell bodies have to be either located on the electrodes or at their very close vicinity, at least closer than 10 μm . By using circular poly-lysine domains of 70 μm in diameter centered on the 30- μm electrodes, we are then sure that if a cell body is on the chemical pattern, its distance to the recording electrode is less than 10–20 μm . Therefore, the use of a chemical pattern with the MEA offers two main advantages depending on the plating density: (1) more electrodes have at least one neuron in close vicinity; (2) more electrodes can have at most one neuron at close vicinity. As a consequence the use of MEA with neuronal culture can be envisaged at low and physiological densities with a reasonable amount of electrodes recording single units and will prevent further studies at abnormally high densities.

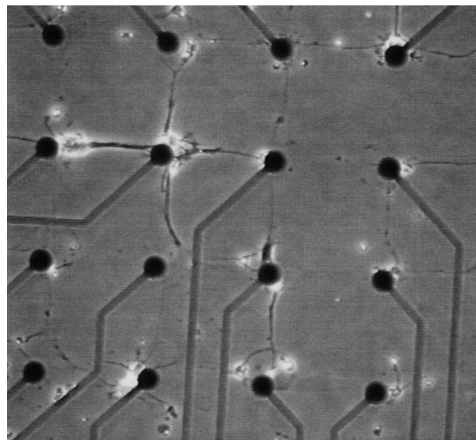
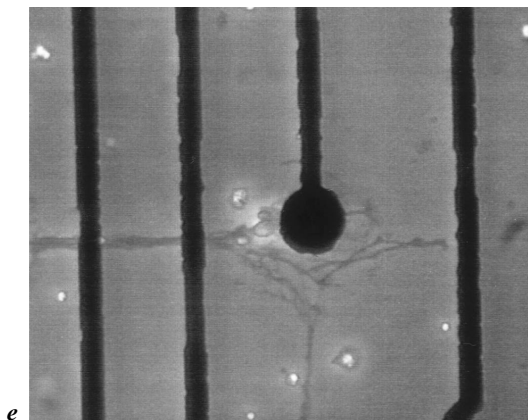
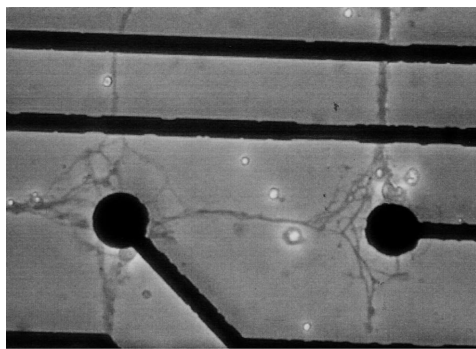
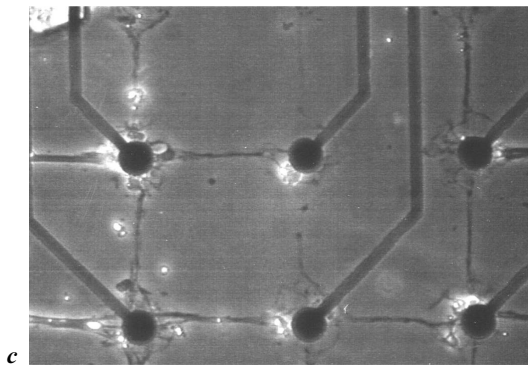
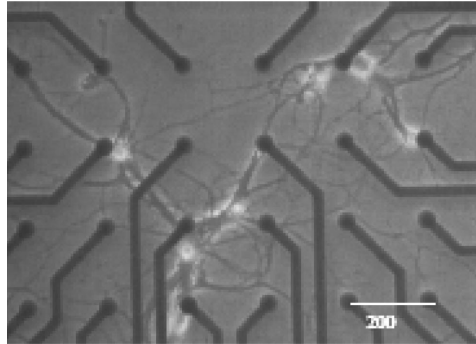
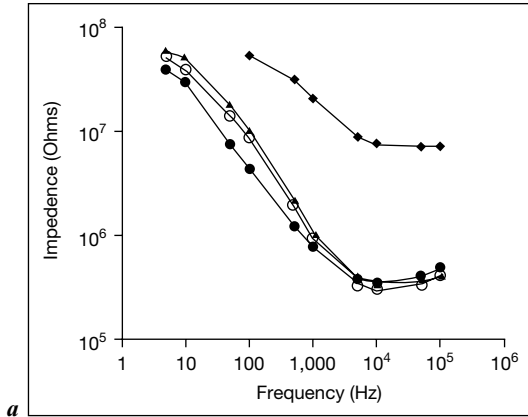


Fig. 14. Patterning MEA by lithography improves their use for single unit recording of a large number of cells in neuronal culture. **a** Module of the impedance of an MEA electrode as a function of the frequency. Black circles = cleaned MEA; black diamonds = silicized

Final Comments

Our protocol is a robust and accessible way to produce *mature, ordered* neuronal networks with intact neuronal physiology. For at least 5 weeks, the geometry of the network and the membrane properties of both excitatory and inhibitory cells are maintained and functionally mature synapses are formed. Several observations indicate that the inhibitory and excitatory synapses are mature: (1) existence of clusters of presynaptic markers, (2) specific localization of inhibitory and excitatory synapses; (3) voltage clamp recordings of spontaneous EPSCs and inhibitory post synaptic currents or IPSCs with standard current kinetics and pharmacology. The synaptic connectivity between pairs of neurons and the spontaneous activity are similar to what has been observed between pyramidal neurons in slices [45, 41] and may reflect a general property of neuronal network organization.

Moreover, as shown in this paper, the synaptic connectivity of a network can easily be assayed and appears to be constrained by the geometry. Because of the simplicity of the identification and study of given connected neurons, we believe that our technique may constitute a novel tool for long-term observation of the interactions between multiple neurons in a network.

Our technique produces about a hundred networks per glass coverslip in a defined medium. The main advantages of these neuronal chips are the fixed number and position of the cellular bodies, the proper maturation of the neurons, the simplicity of the statistically known connectivity patterns, and finally the possible long-term maintenance of the networks in a serum-free medium. We have also shown that by identifying a posteriori the position of inhibitory cells with an immunocytochemical staining in a given network, we can estimate most of the relevant parameters of the architecture of the network (i.e., number of total interconnected cells, probability of connection, and the nature of the connections). These properties could be of great interest to systematically screen new pharmacological compounds at different stages of neuronal development.

Simplicity of Fabrication, Reproducibility, and Application to Other Cell Types

The photolithography protocol requires little equipment. The lithography masks, which can be obtained commercially, can be designed using a simple

MEA; hollow circles = plasma etched silanized MEA; black triangles = poly-lysine-coated MEA. **b-f** Rat hippocampal neurons culture on a MEA after 7 days in vitro; **b** without chemical pattern; **c-f** with a chemical pattern consisting of circular poly-lysine domains (70 μm in diameter) on the electrodes and thin poly-lysine lines (width less than 10 μm) between them. The circular electrodes are separated by 200 μm .

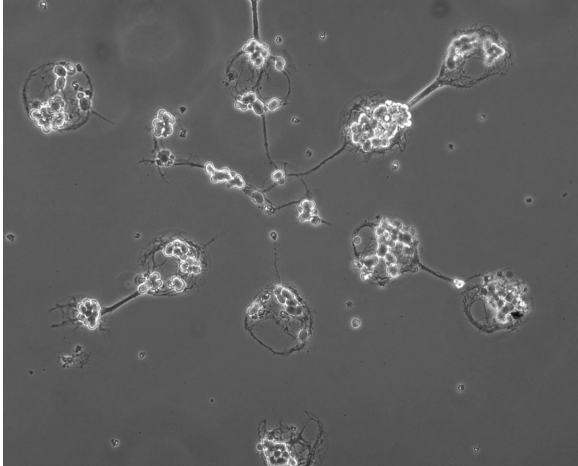


Fig. 15. The lithography protocol can be applied to other cell types, as shown here with retinal cells. Retinal cells (2 days after plating on this DIC image) are growing on the poly-lysine domains only. This preliminary experiment has been performed with Frank Pfrieder (Centre de Neurochimie, Strasbourg) with a high density of cells to test if the adhesion patterns were guiding the growth of the cells.

optical setup based on a commercial fluorescence microscope and a thermal evaporator. Our protocol is reproducible and works systematically when coupled with a robust, widely used primary culture protocol [17]. The two main conditions for the long-term persistence of adhesion patterns are the absence of serum in the maintenance medium and the presence of an anti-mitotic agent (AraC). If these conditions are met, our protocol can be used for different cell types. For example, with Franck Pfrieder (Centre de Neurochimie, Strasbourg), we have performed successful tests with retinal neurons from rat embryos (see fig. 15).

Functional Structure of a Network

The functional structure of a network refers to the nature and cellular properties of each neuron as well as the synaptic connections between them. We have studied how various lithography-controlled architectures determine characteristics of the resultant functional structure. We have demonstrated that the functional structure of our networks depends on (1) the total number of neurons, (2) the nature (GABAergic or glutamatergic) of the neurons and (3) their relative positions, corresponding to connection probabilities and efficiencies.

Total Number of Neurons

Controlled architecture neuronal networks are isolated: the number of neurons is fixed from plating until the day the experiment is performed. In the networks we designed, the number of neurons varied from one to twenty but the possibility of producing large patterns allows building networks with thousands of neurons.

Neuron Nature

The glutamatergic/GABAergic nature of each neuron can be resolved a posteriori by immunocytochemistry or during the experiment with single patch clamping since neurons always form autapses. The neuron nature is also a fixed parameter in a given network. Inhibitory neurons constitute between 10 and 20% of all neurons in our culture. Thus the inhibition/excitation balance is between 0 and 0.2. Our protocol is a new way to study the impact of a variable inhibition/excitation balance on the generation of rhythms in spontaneous or evoked electrical activity [46].

Connectivity and Geometry

As we have seen, the distance between two given glutamatergic neurons in a network corresponds to a probability and efficiency of connection (estimated by the amplitude of the EPSC). The physical distance between neurons in the network is associated with a decreasing probability of synaptic contacts. Our controlled architecture neuronal networks are comparable to interconnected autapses with a connection probability decreasing with distance (see fig. 15).

A New Tool to Study the Interaction of Neurons during Development

Because of the lack of fixed marks on glass coverslips, it is difficult in culture to identify a single cell or subnetwork in experiments performed on the same network over several days. To recognize a given cell, some labs have developed a press system to print a matrix on plastic dishes. But even this system is inadequate because of the mobility of neurons on glass coverslips. As we have shown with our protocol using time lapse microscopy, cell bodies do not leave the poly-lysine domains. With the photolithography protocol that we have designed, one can easily recognize and follow several cells for weeks in vitro.

A second advantage of our system, for those interested in studying neuron interaction during development, is the fact that neighboring neurons are highly connected. This feature may facilitate the physiological studies of synapses in vitro during development as well as the effect of chronic treatments [1, 2].

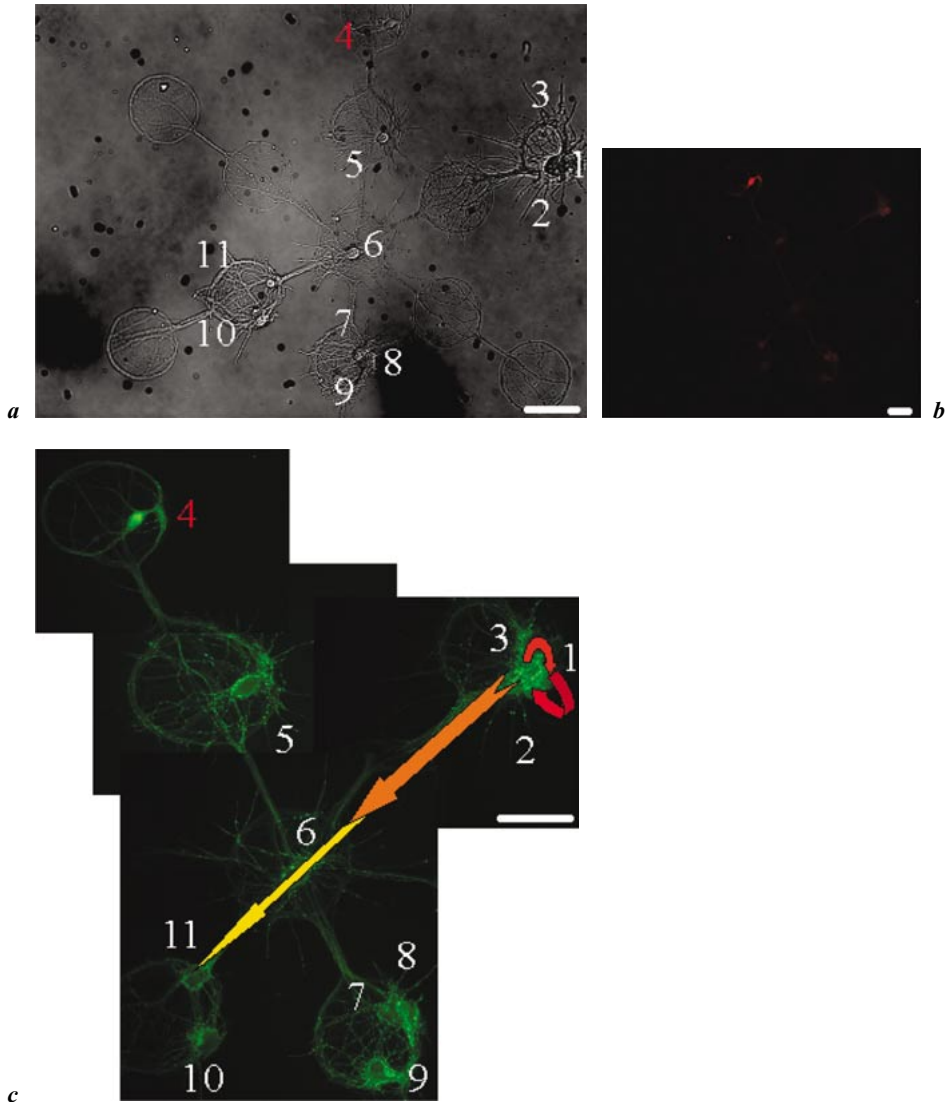


Fig. 16. Functional structure of a typical network of controlled architecture including eleven neurons with a star geometry (20 days in vitro). **a** DIC (differential interference contrast) image of a controlled architecture neuronal network with a star geometry. The total number of neurons (11) and their respective position is constant in time. **b, c** A posteriori, using immunocytochemistry with antibodies directed against GABA (red, **b**) and GAD 65 (green, **c**), the number and the position of GABAergic cells can be evaluated. In this example, only one neuron is GABAergic: neuron 4. It has formed GAD 65 positive synapses on all the surrounding glutamatergic neurons in the network. **c** The probability of synaptic contacts between two

Finally, developmental studies require long-term measurements of activity. These studies can be performed using calcium imaging with successive staining. However, the possibility to achieve the coupling with MEA techniques may resolve most of the problems encountered when one is interested in recording and stimulating many single cells in a given network with good spatial and temporal resolution [43], and performing such an experiment several days in a row.

Perspectives

The next major breakthrough would be to design a new protocol based on the original one that allows several successive lithographies on the same pattern. This would lead to several new developments, such as grafting different type of molecules (more than two!) onto the substrate, which could favor further refinements of constructed networks. One could then plan to orient inhibitory or excitatory cell adhesion or to favor axonal or dendritic growth.

Finally, since our protocol has succeeded in producing patterns with nondividing cells (neurons) as well as dividing cells (astrocytes), it opens the possibility of forming hybrid assemblies and studying specific interactions between different types of mammalian cells (such as motoneurons and muscular fibers or tumor and nontumor cells considered to be easier to maintain *in vitro*).

Acknowledgements

This work has been supported by the ‘Université Louis Pasteur, Strasbourg’ (contrat exceptionnel 2001), the ‘Ministère de la Recherche’ (ACI jeune chercheur 1999), the CNRS (Projet jeune chercheur 1999 and ATIP jeune chercheur 2002, département SPM) and the DRET (contrat n° 961179, 1996). The time lapse setup has been founded by the ‘Conseil Régional d’Alsace’, the ‘Fondation pour la Recherche Médicale’ and the CNRS. We thank Emmanuel Jover for his help in using the time lapse microscope and Caglar Girit for his invaluable comments on the manuscript.

neurons depends on the distance between them in 3-week-old neuronal networks. This probability P_c is schemed by arrows for the neuron called 1. P_c is maximum (red arrow) for autapses and synapses formed on neurons of the same disk (neurons 2 and 3). P_c decreases for first neighboring neurons (neuron 6, orange arrow) and second neighbors (neurons 11, 10, 7, 8, 9 and 5, yellow arrow represented towards the neuron 11). Scale bar = 50 μm .

References

- 1 Turrigiano G, Abbott LF, Marder E: Activity-dependent changes in the intrinsic properties of cultured neurons. *Science* 1994;264:974–977.
- 2 Turrigiano GG, Leslie KR, Desai NS, Rutherford LC, Nelson SB: Activity-dependent scaling of quantal amplitude in neocortical neurons. *Nature* 1998;391:892–896.
- 3 Prinz AA, Fromherz P: Electrical synapses by guided growth of cultured neurons from the snail *Lymnaea stagnalis*. *Biol Cybern* 2000;82:L1–L5.
- 4 Zeck G, Fromherz P: Noninvasive neuroelectronic interfacing with synaptically connected snail neurons immobilized on a semiconductor chip. *Proc Natl Acad Sci USA* 2001; 98:10457–10462.
- 5 Craig AM, Banker G, Chang W, McGrath ME, Serpinskaya AS: Clustering of gephyrin at GABAergic but not glutamatergic synapses in cultured rat hippocampal neurons. *J Neurosci* 1996;16:3166–3177.
- 6 Fitzsimonds RM, Song HJ, Poo MM: Propagation of activity-dependent synaptic depression in simple neural networks. *Nature* 1997;388:439–448.
- 7 Rao A, Craig AM: Activity regulates the synaptic localization of the NMDA receptor in hippocampal neurons. *Neuron* 1997;19:801–812.
- 8 Gomperts SN, Rao A, Craig AM, Malenka RC, Nicoll RA: Postsynaptically silent synapses in single neuron cultures. *Neuron* 1998;21:1443–1451.
- 9 Rao A, Kim E, Sheng M, Craig AM: Heterogeneity in the molecular composition of excitatory postsynaptic sites during development of hippocampal neurons in culture. *J Neurosci* 1998; 18:1217–1229.
- 10 Bi G, Poo M: Synaptic modification by correlated activity: Hebb's postulate revisited. *Annu Rev Neurosci* 2001;24:139–166.
- 11 Xiang Y, Li Y, Zhang Z, Cui K, Wang S, Yuan XB, Wu CP, Poo MM, Duan S: Nerve growth cone guidance mediated by G protein-coupled receptors. *Nat Neurosci* 2002;5:843–848.
- 12 Tsodyks M, Kenet T, Grinvald A, Arieli A: Linking spontaneous activity of single cortical neurons and the underlying functional architecture. *Science* 1999;286:1943–1946.
- 13 Cossart R, Aronov D, Yuste R: Attractor dynamics of network UP states in the neocortex. *Nature* 2003;423:283–288.
- 14 Kenet T, Bibitchkov D, Tsodyks M, Grinvald A, Arieli A: Spontaneously emerging cortical representations of visual attributes. *Nature* 2003;425:954–956.
- 15 Cohen I, Miles R: Contributions of intrinsic and synaptic activities to the generation of neuronal discharges in *in vitro* hippocampus. *J Physiol* 2000;524:485–502.
- 16 Wang XJ: Synaptic reverberation underlying mnemonic persistent activity. *Trends Neurosci* 2001;24:455–463.
- 17 Banker G, Goslin K: Developments in neuronal cell culture. *Nature* 1988;336:185–186.
- 18 Goslin K, Banker G: Experimental observations on the development of polarity by hippocampal neurons in culture. *J Cell Biol* 1989;108:1507–1516.
- 19 Bi G, Poo M: Distributed synaptic modification in neural networks induced by patterned stimulation. *Nature* 1999;401:792–796.
- 20 Lo YJ, Poo MM: Heterosynaptic suppression of developing neuromuscular synapses in culture. *J Neurosci* 1994;14:4684–4693.
- 21 van den Pol AN, Obrietan K, Belousov AB, Yang Y, Heller HC: Early synaptogenesis *in vitro*: Role of axon target distance. *J Comp Neurol* 1998;399:541–560.
- 22 Offenhausser A, Sprossler C, Matsuzawa M, Knoll W: Field-effect transistor array for monitoring electrical activity from mammalian neurons in culture. *Biosens Bioelectron* 1997;12:819–826.
- 23 Kleinfeld D, Kahler KH, Hockberger PE: Controlled outgrowth of dissociated neurons on patterned substrates. *J Neurosci* 1988;8:4098–4120.
- 24 Stenger DA, Hickman JJ, Bateman KE, Ravenscroft MS, Ma W, Pancrazio JJ, Shaffer K, Schaffner AE, Cribbs DH, Cotman CW: Microlithographic determination of axonal/dendritic polarity in cultured hippocampal neurons. *J Neurosci Methods* 1998;82:167–173.
- 25 Wheeler BC, Corey JM, Brewer GJ, Branch DW: Microcontact printing for precise control of nerve cell growth in culture. *J Biomech Eng* 1999;121:73–78.

- 26 Ma W, Liu QY, Jung D, Manos P, Pancrazio JJ, Schaffner AE, Barker JL, Stenger DA: Central neuronal synapse formation on micropatterned surfaces. *Brain Res Dev Brain Res* 1998;111: 231–243.
- 27 Matsuzawa M, Tabata T, Knoll W, Kano M: Formation of hippocampal synapses on patterned substrates of a laminin-derived synthetic peptide. *Eur J Neurosci* 2000;12:903–910.
- 28 Scholl M, Sprossler C, Denyer M, Krause M, Nakajima K, Maelicke A, Knoll W, Offenhausser A: Ordered networks of rat hippocampal neurons attached to silicon oxide surfaces. *J Neurosci Methods* 2000;104:65–75.
- 29 Ikegaya Y, Itsukaichi-Nishida Y, Ishihara M, Tanaka D, Matsuki N: Distance of target search of isolated rat hippocampal neuron is about 150 micron. *Neuroscience* 2000;97:215–217.
- 30 Evans MS, Collings MA, Brewer GJ: Electrophysiology of embryonic, adult and aged rat hippocampal neurons in serum-free culture. *J Neurosci Methods* 1998;79:37–46.
- 31 Staley KJ, Otis TS, Mody I: Membrane properties of dentate gyrus granule cells: Comparison of sharp microelectrode and whole-cell recordings. *J Neurophysiol* 1992;67:1346–1358.
- 32 Wyart C, Ybert C, Bourdieu L, Herr C, Prinz C, Chatenay D: Constrained synaptic connectivity in functional mammalian neuronal networks grown on patterned surfaces. *J Neurosci Methods* 2002;117:123–131.
- 33 Pettit DL, Augustine GJ: Distribution of functional glutamate and GABA receptors on hippocampal pyramidal cells and interneurons. *J Neurophysiol* 2000;84:28–38.
- 34 Wilcox KS, Buchhalter J, Dichter MA: Properties of inhibitory and excitatory synapses between hippocampal neurons in very low density cultures. *Synapse* 1994;18:128–151.
- 35 Pickard L, Noel J, Henley JM, Collingridge GL, Molnar E: Developmental changes in synaptic AMPA and NMDA receptor distribution and AMPA receptor subunit composition in living hippocampal neurons. *J Neurosci* 2000;20:7922–7931.
- 36 Smetters D, Majewska A, Yuste R: Detecting action potentials in neuronal populations with calcium imaging. *Methods* 1999;18:215–221.
- 37 Peterlin ZA, Kozloski J, Mao BQ, Tsiola A, Yuste R: Optical probing of neuronal circuits with calcium indicators. *Proc Natl Acad Sci USA* 2000;97:3619–3624.
- 38 Kozloski J, Hamzei-Sichani F, Yuste R: Stereotyped position of local synaptic targets in neocortex. *Science* 2001;293:868–872.
- 39 Mao BQ, Hamzei-Sichani F, Aronov D, Froemke RC, Yuste R: Dynamics of spontaneous activity in neocortical slices. *Neuron* 2001;32:883–898.
- 40 Muramoto K, Ichikawa M, Kawahara M, Kobayashi K, Kuroda Y: Frequency of synchronous oscillations of neuronal activity increases during development and is correlated to the number of synapses in cultured cortical neuron networks. *Neurosci Lett* 1993;163:163–165.
- 41 Feller MB: Spontaneous correlated activity in developing neural circuits. *Neuron* 1999;2: 653–656.
- 42 Hammerle H, Egert U, Mohr A, Nisch W: Extracellular recording in neuronal networks with substrate integrated microelectrode arrays. *Biosens Bioelectron* 1994;9:691–696.
- 43 Jimbo Y, Tateno T, Robinson HP: Simultaneous induction of pathway-specific potentiation and depression in networks of cortical neurons. *Biophys J* 1999;76:670–678.
- 44 Jimbo Y, Kasai N, Torimitsu K, Tateno T, Robinson HP: A system for MEA-based multisite stimulation. *IEEE Trans Biomed Eng* 2003;50:241–248.
- 45 Markram H, Lubke J, Frotscher M, Roth A, Sakmann B: Physiology and anatomy of synaptic connections between thick tufted pyramidal neurones in the developing rat neocortex. *J Physiol* 1997;500:409–440.
- 46 Shu Y, Hasenstaub A, McCormick DA: Turning on and off recurrent balanced cortical activity. *Nature* 2003;423:288–293.

Laurent Bourdieu

Laboratoire de Dynamique des Fluides Complexes, UMR 7506 CNRS

Université Louis Pasteur, Institut de Physique

3, rue de l'Université, FR-67084 Strasbourg (France)

Tel. +33 390 24 06 32, Fax +33 390 24 07 45, E-Mail bourdieu@dfc.u-strasbg.fr